

Liquid: Language Models are Scalable Multi-modal Generators

Junfeng Wu^{1,2}, Yi Jiang^{2,†}, Chuofan Ma^{2,3},
 Yuliang Liu¹, Hengshuang Zhao³, Zehuan Yuan², Song Bai^{2,*}, Xiang Bai^{1,*}

¹Huazhong University of Science and Technology ²Bytedance Inc

³University of Hong Kong

wjf5203@gmail.com, jiangyi.enjoy@bytedance.com,

b20mcf@connect.hku.hk, ylliu@hust.edu.cn, hszhao@cs.hku.hk

yuanzehuan@bytedance.com, songbai.site@gmail.com, xbai@hust.edu.cn

Abstract

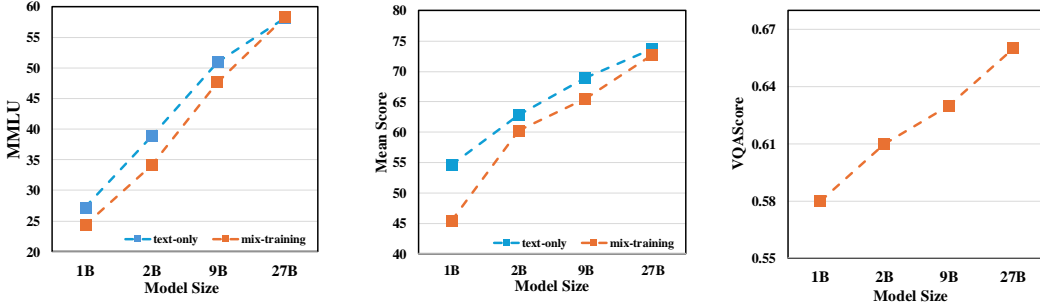
We present Liquid, an auto-regressive generation paradigm that seamlessly integrates visual comprehension and generation by tokenizing images into discrete codes and learning these code embeddings alongside text tokens within a shared feature space for both vision and language. Unlike previous multimodal large language model (MLLM), Liquid achieves this integration using a single large language model (LLM), eliminating the need for external pretrained visual embeddings such as CLIP. For the first time, Liquid uncovers a scaling law that performance drop unavoidably brought by the unified training of visual and language tasks diminishes as the model size increases. Furthermore, the unified token space enables visual generation and comprehension tasks to mutually enhance each other, effectively removing the typical interference seen in earlier models. We show that existing LLMs can serve as strong foundations for Liquid, saving 100 \times in training costs while outperforming Chameleon in multimodal capabilities and maintaining language performance comparable to mainstream LLMs like LLAMA2. Liquid also outperforms models like SD v2.1 and SD-XL (FID of 5.47 on MJHQ-30K), excelling in both vision-language and text-only tasks. This work demonstrates that LLMs such as LLAMA3.2 and GEMMA2 are powerful multimodal generators, offering a scalable solution for enhancing both vision-language understanding and generation. The code and models will be released.

1 Introduction

The recent advancement of Large Language Models (LLMs) [4, 63, 8, 47, 64, 60] has sparked a trend of extending the foundational capabilities of LLMs to the visual domain, giving rise to Multi-modal Large Language Models (MLLMs) [38, 76, 36, 41, 5, 37]. In the realm of visual understanding, MLLMs such as LLaVA [38] typically adopt the pretrained CLIP [45] model as the visual tokenizer, followed by a two-stage training process to align the vision-and-language feature space. While for text-guided visual generation, most MLLMs [18, 19, 25, 58, 57] rely on an external diffusion model to generate images. Despite these methods have achieved remarkable multi-modal understanding and generation performances, the use of external visual modules introduces additional architecture complexity to the system, and potentially poses a bottleneck when scaling up the LLMs.

In light of the aforementioned issues, an emerging line of research [15, 49, 12, 71, 62, 56] attempts to employ the VQVAE [65, 15] model as a universal visual tokenizer for MLLMs. Analogous to

*Corresponding authors: <xbai@hust.edu.cn>, <songbai.site@gmail.com>; †: project lead



(a) MMLU zero-shot performance (b) Mean score of language tasks (c) VQAScore in GenAI-Bench

Figure 1: The performance impact of multi-modal mixed training versus text-only training on language tasks. Figure (a) compares the performance of both methods on MMLU (zero-shot), while Figure (b) shows the average scores on 5 language tasks, including HellaSwag, WinoGrande, ARC-Easy, ARC-Challenge, and BoolQ. It can be seen that multi-modal mixed training does impact language performance when the model size is small. However, this degradation gradually disappears as the model size increases, demonstrating that larger LLMs have greater capacity to learn visual generation without impacting the model’s original capabilities. Figure (c) demonstrates that the image generation capabilities of the model are continuously improved as the model size increases. We report the VQA score on the advanced prompts set of GenAI-Bench.

the role played by the BPE [53] tokenizer in LLMs, VQVAE establishes a bi-directional mapping between raw pixels and discrete codes. This enables the MLLMs to learn visual code embeddings jointly with text tokens, rather than constrained by the feature space of a pretrained visual encoders like CLIP or pretrained visual generators like diffusion models. Moreover, the discrete nature of visual tokens allows uniform modeling of visual and text tokens with the same next-token prediction loss, which seamlessly integrates both modalities. LWM [39] and Chameleon [59] are the pioneers in exploring this approach. However, these methods involve extensive training from scratch, which makes it computationally expensive to disseminate exploration in this form. Follow-up works further introduces bi-directional attention [75], discrete diffusion modeling [69], and residual codes [68] to handle visual tokens. Although these techniques improve the performance in visual generation and understanding, they unavoidably impose discrepancies in vision and language modeling.

In this paper, we revisit the plain design of MLLMs and present Liquid, a scalable decoder-only architecture for multi-modal generation and understanding. We employ the VQVAE [15] model as the visual tokenizer to encode images into discrete codes, which share the same vocabulary and embedding space with text tokens. Such a strategy ensures that Liquid can benefit from the mature structure designs and acceleration techniques of LLMs. We find that existing LLMs are excellent starting points for training, as they have already acquired strong semantic understanding and generation capabilities. We directly build our model on existing LLMs [60, 61, 14, 24] and stick with the original structure of LLMs, solely expanding their vocabulary size to accommodate the image token indices derived from VQVAE. We employ both text-only and image-text pair data to conduct multi-modal mixed training on Liquid, thereby enabling it to simultaneously continue functioning on text-only tasks, image understanding tasks, and text-guided image generation tasks. Compared to Chameleon [59], which is trained from scratch on massive amounts of low-quality data, we continue training existing LLMs on a smaller amount of high-quality data to equip them with visual understanding and generation capabilities. This approach saves 100 \times of training cost while achieving stronger multimodal capabilities and maintains language capabilities comparable to mainstream LLMs.

We further explore the scaling property and performance of Liquid with different scales of LLMs. We find that when visual and language tasks are trained in a unified space, smaller models experience a performance drop in the original language tasks and perform worse in visual generation tasks compared to models trained solely on visual generation. However, as the model size increases, the performance trade-off gradually disappears. This phenomenon demonstrates that larger LLMs have sufficient capacity to handle both visual generation and language tasks simultaneously. This highlights the scaling advantage of utilizing LLMs directly for image generation. To our knowledge,



Figure 2: The generated samples from Liquid-7B, showcase excellent capabilities in crafting high aesthetic and described-consistent images.

no previous works have studied the impact of unifying these tasks in an auto-regressive form. Notably, through data ablation experiments, we discover that the training of visual understanding and visual generation can mutually boost each other under the framework of the Liquid. It further confirms the tremendous potential of unifying visual generation and understanding tasks into LLMs.

We evaluate the capabilities of Liquid across text-guided image generation, visual understanding, and general text-only tasks. For image generation, Liquid outperforms other auto-regressive based models, as well as some diffusion models like SD-XL and achieve FID of 5.47 on MJHQ-30K, demonstrating that LLMs can acquire excellent imagery capabilities efficiently with a limited amount of data. For visual understanding, Liquid surpasses Chameleon and achieved results comparable to those of well-established MLLMs. In text-only tasks, Liquid achieves comparable performance with Chameleon, which used mix pre-training on a very large scale, and surpasses the performance of LLAMA2, demonstrating undegraded linguistic capabilities.

In summary, the main contributions of this paper can be categorized into the following points:

- An efficient decoder-only multi-modal generation framework that seamlessly carries out visual generation, visual comprehension, and pure language tasks.
- Comprehensive experiments about scaling laws of unified multi-modal models, revealing that the trade-off between language and visual tasks diminishes as scale of model increases, thereby proving the applicability of the appealing properties of LLMs.

- An insightful discovery regarding the mutual boost of visual understanding and generation tasks within LLMs through the unification of visual tokens, highlighting the potential of LLMs to improve both understanding and generation capabilities by mixtraining.

2 Related Work

Multi-modal Large Language Models. The rapid advancement of Large Language Models (LLMs) [8, 4, 63, 64, 60] in recent years has inspired researchers to explore their application in visual understanding tasks. The integration of visual information with language models brings about potent multi-modal comprehension and reasoning abilities. Initial works such as LLaVA [38] and MiniGPT4 [76] propose to project features from a pre-trained visual foundation model [45, 30] into the feature space of LLMs, exhibiting encouraging multi-modal understanding capacities. Building upon this progress, an array of MLLMs [1, 29, 11, 2] have been well-designed and extensively trained on comprehensive vision-language data, achieving noteworthy performance on visual understanding and reasoning tasks. The LLaVA series [38, 36, 41, 5, 7, 37, 32] employ image-text pair data to train a projector, projecting the image-feature from CLIP to align the language spaces within the input space of LLMs. They further enhance visual understanding and reasoning abilities by training the entire pipeline via a curated multi-modal instruction tuning dataset. Despite their robust multi-modal understanding capabilities, existing models are primarily focused on visual understanding, falling short on generating visual outputs that extend beyond text.

Vision Generation. In the past few years, the realm of visual generation has been primarily dominated by diffusion models [44, 50, 46, 34, 48], which progressively generate high-quality, high-resolution images via a diffusion process over a continuous latent space. Several efforts [18, 19, 25, 58, 57, 66] have attempted to extend LLMs with pretrained diffusion models to integrate image generation capabilities. These studies employ diffusion models as a tool where the diffusion models generate images conditioned on the features output by the LLMs. In this combination, LLMs merely contribute the semantic feature output and lack the direct ability to generate visual content. Moreover, the upper limit of visual generation capacity is dictated by the pre-trained diffusion model, leaving the inherent potential of LLMs in visual generation under-explored.

An alternative viable approach involves using autoregressive models to generate images by predicting the next token in a sequence, as exemplified by models like DALL-E [49], CogView [12], Parti [71] and LlamaGen [56]. Visual AutoRegressive modeling (VAR)[62] redefined auto-regressive learning on images as coarse-to-fine “next-scale prediction”. It demonstrates superior generalization and scaling capabilities compared to diffusion transformers while requiring fewer steps. These models typically employ VQVAE [15] to tokenize images into a set of discrete codes, subsequently training a decoder-only transformer to predict image codes which are then detokenized back to images. These approaches showcase the potential of decoder-only LLMs in directly conducting image generation. However, they often fail to match the performance of diffusion models and do not explore the possibility of unified output between visual and linguistic modalities. In this work, our objective is to enable LLMs to generate visual content via next-token prediction without altering their structure or capabilities, and explore the characteristics that emerge from the combination of these two tasks within LLMs.

Unified Multimodal Understanding and Generation Several early efforts have explored how to construct a unified multi-modal large model for visual generation and understanding based on LLMs. The central challenge lies in tokenizing images into sequence inputs for the LLMs and detokenizing the sequential output of the LLMs back into images, the choice of image tokenizer. Some methods [18, 19, 58, 57] use vision encoders based on ViT like CLIP to encode images into continuous feature maps. The continuous visual space from CLIP can retain more visual information and have a pre-trained, aligned space with language feature. However, the continuous feature often necessitates an additional diffusion module for image detokenization. Other works [39, 59, 68] employ VQVAE to encode images into discrete tokens and train LLMs to predict them. Still other works [40, 69, 67] use both ViT and VQVAE as tokenizers to garner their benefits. Discrete image features can share the same embedding space with text input, permitting joint reasoning over both modalities within a unified architecture without the requirement for modality-specific components. It is beneficial for model scale-up. Consequently, in our work, we choose VQVAE as the sole image tokenizer. Our work is most similar to LWM [39] and Chameleon [59]. However, they display inferior image understanding and generation capabilities, and need extensive large scale multi-modal

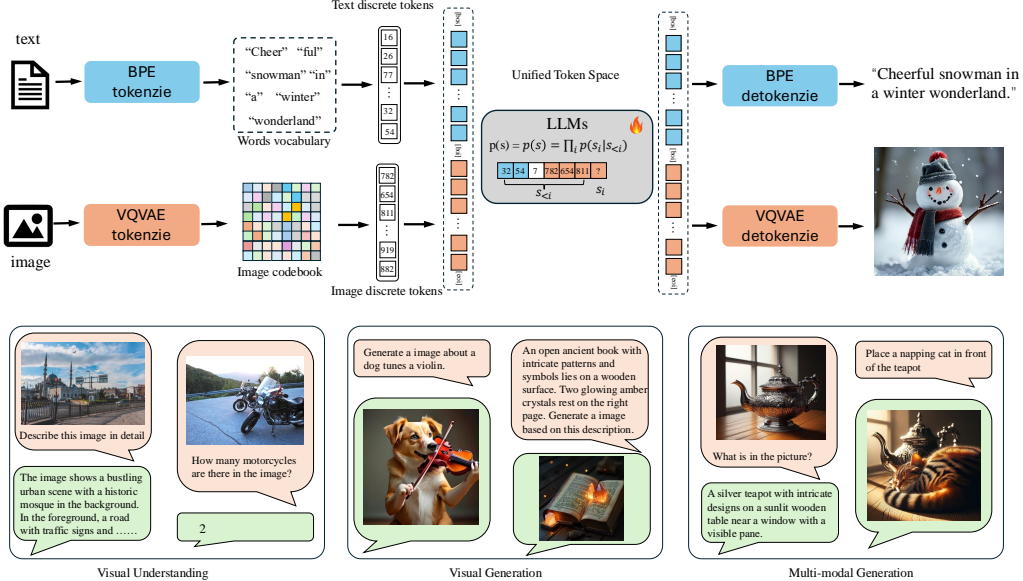


Figure 3: Pipeline of Liquid. The structure of Liquid follows a consistent format that treats images in the exact same way as text. A VQVAE based image tokenizer transforms the input images into discrete codes, which share the same vocabulary and embedding space with text codes. The image tokens and text tokens, once mixed, are fed into the LLMs and trained in the form of next token prediction. The lower part of the figure demonstrates that Liquid can handle various multi-modal understanding and generation tasks.

pre-training, which is a significant burden. In contrast, we propose to start from any existing LLMs and enhance their visual understanding and generation abilities by continuing training with a small amount of high-quality data, without altering any model structures.

3 Method

3.1 Image Tokenizer

We use the same tokenizer as Chameleon [59], which is a VQGAN [15]. It encodes a 512×512 image into 1024 discrete tokens in a codebook of size 8192. We appended these discrete image tokens to the text codebook produced by the BPE [53] tokenizer to expand the vocabulary size of the LLM, thereby extending its language space to a multi-modal space encompassing both visual and linguistic elements. To speed up training, we use this tokenizer to pre-convert all images used during training into discrete tokens.

3.2 Architecture

As illustrated in Fig. 3, Liquid can be constructed based on any existing large language models (LLMs). In this paper, we employ the GEMMA-7B [60] and GEMMA-2 series [61] as the base model of Liquid. We refrain from altering any structures within the LLMs to facilitate continued training directly from pre-trained weights. The only modification is the addition of 8192 new learnable embeddings for discrete image tokens. Correspondingly, we extend the original LM head by 8192 dimensions to enable the model to predict both text and image tokens within the same embedding space. The LLMs maintain their original next-token prediction training objective without any changes, with the only variation being that their vocabulary space has been extended from purely language-space to a combined space for both visual and linguistic modalities.

We use the GEMMA-7B [60] model as our primary model to validate its multimodal understanding, image generation capabilities, and performance on text-only tasks after augmenting it with the ability to understand and generate images. To further investigate whether a trade-off exists when

accommodating visual generation tasks and text generation tasks within the same LLM space, as well as to explore the scaling performance of different sized models, we conducted same training on LLAMA-3 1B [14] and GEMMA-2 series [61] at scales of 2B, 9B, and 27B, thereby observing their distinct performances.

3.3 Data Preparation

3.3.1 Continue Pre-training Data

Text-only data. To maintain the language abilities of pre-trained LLMs, we sample text-only data from public datasets for the pre-training stage. We sample 15M text data from DCLM [28], 12M from SlimPajama [55], and 3M code data from Starcoderdata [31], totaling 30M text instances for approximately 60 billion text tokens in the pre-training stage.

Image-text pairs. We use JourneyDB [43] and internal MidJourney-style synthetic data to compile 30M high-quality image data, for a total of 30 billion image tokens. All the data are used to form a hybrid multi-modal data for continue pre-training, resulting in quick acquisition of decent image generation capabilities while retaining language abilities. Furthermore, we reversed 20% of text-to-image data to train in a captioning format to enhance its understanding of images.

3.3.2 Instruction Tuning Data

After the pre-training stage, the model has already attained substantial image generation capabilities and a decent level of image understanding. We use 1M LMSYS [74] as text-only instruction data, coupled with 1M text-to-Image data sampled from high-quality data, and 1.5M multi-modal instruction tuning data introduced in Minigemini [32]. This compiles a 3.5M hybrid instruction tuning data for further refining our model.

3.4 Training Procedure

Data Formulation. During the continue pre-training stage, we define the input format for multi-modal training data as:

$$[\text{bos}] \{ \text{text token} \} [\text{boi}] \{ \text{image token} \} [\text{eof}][\text{eos}] .$$

Here, [bos] and [eos] are the begin-of-sequence and end-of-sequence tokens defined in the original text tokenizer. We incorporate two additional spatial tokens, [boi] and [eof], to specifically signify the start and end of image tokens. All candidate images are filtered based on their aspect ratios, retaining those with a ratio smaller than 2, and after center cropping, they are resized to 512×512 pixels. With the image tokenizer, each image has a token length of 1024. During the instruction tuning stage, we construct a series of prompts to guide the model to generate images and randomly select from these during each training iteration.

Training Objective. Since all images are tokenized into discrete image tokens that share the same vocabulary and embedding space as text tokens, the training objective is wholly consistent with LLMs via next-token prediction and utilizes the standard cross-entropy loss. Moreover, we observe that during the continue pre-training stage, models of 7B size and above tend to encounter loss spikes in the early stages of training. It significantly impacts the training performance and convergence speed. To mitigate this issue, we reduce the max grad norm to 0.5 for larger models and use max-z loss [70] to normalize the logits, enhancing the stability of training.

Training Details. In all experiments, we initiate with a learning rate of 2e-5. Except for the scaling experiments that employed a constant learning rate, all other tests utilized a cosine learning schedule. The training batch size is set at 1024, and the max context length is set to 2048. We use the DeepSpeed Zero3 optimization strategy.

4 Experiments

4.1 Training Details and Evaluation Setting

As Liquid extends the base capabilities of LLMs to generate and understand images, we validate its performance across three aspects: text-guided image generation, visual understanding, and general text-only capabilities.

For the image generation tasks, we evaluate the model on two benchmarks, GenAI-Bench [35] and MJHQ-30K [27]. GenAI-Bench is an challenging image-to-text generation benchmark designed to evaluate the capabilities of visual generation models. It evaluates both basic skills, such as understanding attributes, scenes, and relations in text inputs, and advanced skills, including abilities like counting, differentiation, comparison, and understanding logical relationships from text input, thereby highlighting the graded progression in complexity. GenAI-Bench employs VQAScore, which leverages a visual-question-answering (VQA) model. This enables more precise evaluation of how well the generated image aligns with the text prompt, critically assessing the capability to parse scenes, objects, attributes, relationships, and engage in higher-order reasoning such as comparison and logic. The latter calculates the Frechet Inception Distance (FID) [22] score between the generated images and 30K high-quality images to assess the quality of the generated images.

To evaluate the visual understanding capabilities, we report results on widely-adopted zero-shot image-based benchmarks, which include VQA-v2 [20], GQA [23], TextVQA [54], MME [16].

To validate whether acquiring image understanding and generation capabilities has any impact on the original language abilities of the LLMs, we report overall zero-shot performance across a suite of popular benchmarks that measure commonsense reasoning and reading comprehension capabilities: HellaSwag [73], WinoGrande [51], ARC-Easy [10], ARC-Challenge [10], OpenBookQA [42], PIQA [3], SIQA [52], and BoolQ [9]. We also perform an evaluation of the 5-shot results on MMLU [21], a comprehensive benchmark that measures world/in-domain knowledge and problem-solving skills across 57 subjects.

4.2 Visual Generation Results

As shown in Tab. 2, compare with other auto-regressive based methods, Liquid achieves a better overall score under both basic prompts and advanced prompts. This suggests that the images generated by Liquid align better semantically with the input text prompts. Notably, Liquid also outperforms some well-established diffusion models like SD v2.1 [50] and SD-XL[44] for both basic and advanced prompts. Compared to these diffusion models, Liquid utilizes significantly fewer image data, which indicating that learning based on LLMs can assist the model in understanding the semantic association between the generated content and prompts, while also offering higher training efficiency. Moreover, it demonstrates that LLMs have strong potential for generating complex visual content.

In Tab. 1, we report FID on MJHQ-30K to compare the images quality generated by Liquid with other models. It is observable that Liquid not only has a lower FID than all other auto-regressive methods but also surpasses most well-known diffusion models except Playground v2.5 [27]], achieving a very low FID of 5.47. It indicates that LLMs are also capable of generating high-quality images, as shown in Fig. 2, providing proof that the upper limit of LLMs in terms of image aesthetic quality is not inferior to diffusion models.

Due to the LLMs' capability to output dynamically-length text in the form of next-token prediction, the convenience can be applied to visual generation. We find that by appending instructions about the resolution to the input text prompt, such as "length is: width is:", the model can quickly learn to generate the corresponding code according to the specified number of rows and columns. Fig. 2 demonstrates the generation results at various resolutions, showcasing the flexibility of Liquid.

4.3 Vision-Language Understanding

To validate the vision-language understanding capabilities of Liquid after instruction tuning, we test our model across various public vision-language benchmarks, as shown in Tab. 3. Compare

Table 1: Comparison with other visual generation methods on MJHQ-30K evaluation benchmark. The FID of Liquid is lower than that of all the auto-regressive models and even outperforms most diffusion models. This indicates that the images generated by Liquid have superior aesthetic quality.

Method	Type	#Images	FID \downarrow
SD-XL [44]	Diffusion	2000M	9.55
PixArt [6]	Diffusion	25M	6.14
Playground v2.5 [27]	Diffusion	–	4.48
Show-o [69]	Discrete Diff.	36M	15.18
LWM [39]	Autoregressive	–	17.77
VILA-U (256) [68]	Autoregressive	15M	12.81
VILA-U (384) [68]	Autoregressive	15M	7.69
Janus [67]	Autoregressive	–	10.10
Ours	Autoregressive	30M	5.47

Table 2: Comparison of VQAscore with other visual generation methods on GenAI-Bench. The basic prompts primarily focus on aspects such as scene, attribute, and relation, while the advanced prompts place a greater emphasis on counting, comparison, differentiation, and logic. The advanced prompts require complex visio-linguistic reasoning and present a significantly higher level of difficulty. Liquid outperforms all auto-regressive unified MLLMs on both types of prompts and has even surpassed some well-established diffusion models like SD v2.1 [50] and SD-XL [44]. It demonstrates that the images generated by Liquid align well with the input text prompts.

Method	Type	#Training Images	Attribute↑	Scene↑	Relation↑			Overall↑
					Spatial	Action	Part	
SD v2.1 [50]	Diffusion	2000M	0.80	0.79	0.76	0.77	0.80	0.78
SD-XL [44]	Diffusion	2000M	0.84	0.84	0.82	0.83	0.89	0.83
Midjourney v6 [46]	Diffusion	–	0.88	0.87	0.87	0.87	0.91	0.87
DALL-E 3 [34]	Diffusion	–	0.91	0.90	0.92	0.89	0.91	0.90
Show-o [69]	Discrete Diff.	36M	0.72	0.72	0.70	0.70	0.75	0.70
LWM [39]	Autoregressive	–	0.63	0.62	0.65	0.63	0.70	0.63
VILA-U [68] (256)	Autoregressive	15M	0.78	0.78	0.77	0.78	0.79	0.76
VILA-U [68] (384)	Autoregressive	15M	0.75	0.76	0.75	0.73	0.75	0.73
Ours	Autoregressive	30M	0.84	0.86	0.81	0.83	0.91	0.83

(a) VQAScores on *basic* prompts of GenAI-Bench

Method	Type	#Training Images	Count↑	Differ↑	Compare↑	Logical↑		Overall↑
						Negate	Universal	
SD v2.1 [50]	Diffusion	2000M	0.68	0.70	0.68	0.54	0.64	0.62
SD-XL [44]	Diffusion	2000M	0.71	0.73	0.69	0.50	0.66	0.63
Midjourney v6 [46]	Diffusion	–	0.78	0.78	0.79	0.50	0.76	0.69
DALL-E 3 [34]	Diffusion	–	0.82	0.78	0.82	0.48	0.80	0.70
Show-o [69]	Discrete Diff.	36M	0.70	0.62	0.71	0.51	0.65	0.60
LWM [39]	Autoregressive	–	0.59	0.58	0.54	0.49	0.52	0.53
VILA-U [68] (256)	Autoregressive	15M	0.70	0.71	0.74	0.53	0.66	0.64
VILA-U [68] (384)	Autoregressive	15M	0.68	0.67	0.71	0.51	0.64	0.61
Ours	Autoregressive	30M	0.76	0.73	0.74	0.46	0.74	0.65

(b) VQAScores on *advanced* prompts of GenAI-Bench

Table 3: Comparison with leading methods on visual language benchmarks. * indicates that images in the training split of these datasets are observed during training. “Und.” and “Gen.” denote “understanding” and “generation”. Our performance surpasses most models that unify understanding and generation, and it is comparable with models dedicated to visual understanding in some tasks. † has a longer pre-training phase, can further enhance its performance.

Type	Method	LLM	Visual Token	Res.	VQAv2	GQA	TextVQA	POPE	MME
Und. Only	LLaVA-1.5 [38]	Vicuna-1.5-7B	Continuous	336	78.5*	62.0*	58.2	85.9	1510.7
	VILA [33]	LLaMA-2-7B	Continuous	336	79.9*	62.3*	64.4	85.5	1533.0
	InstructBLIP [11]	Vicuna-7B	Continuous	224	–	49.2	50.1	–	–
	IDEFICS-9B [26]	LLaMA-7B	Continuous	224	50.9	38.4	25.9	–	–
Und. & Gen.	Unified-IO 2 [40]	6.8B from scratch	Continuous	384	79.4*	–	–	87.7	–
	Emu [58]	LLaMA-13B	Continuous	224	52.0	–	–	–	–
	LaVIT [25]	LLaMA-7B	Continuous	224	66.0	46.8	–	–	–
	DreamLLM [13]	Vicuna-7B	Continuous	224	72.9*	–	41.8	–	–
	CM3Leon-7B [72]	7B from scratch	Discrete	256	47.6	–	–	–	–
	LWM [39]	LLaMA-2-7B	Discrete	256	55.8	44.8	18.8	75.2	–
	Show-o [69]	Phi-1.5-1.3B	Discrete	256	59.3*	48.7*	–	73.8	948.4
	VILA-U [39]	LLaMA-2-7B	Discrete	256	75.3*	58.3*	48.3	83.9	1336.2
	Chameleon [59]	34B from scratch	Discrete	512	69.6	–	–	–	–
Ours	Gemma-7B	Discrete	512	68.0*	56.1*	40.4	81.1	1107.2	–
	Ours†	Gemma-7B	Discrete	512	71.3*	58.4*	42.4	81.1	1119.3

with the MLLMs with discrete visual token, Liquid outperforms models with stander VQVAE like LWM [39], Chameleon [59], and Show-o [69], and achieves comparable results with VILA-U [68], which have trained a CLIP based multi-codebook VQVAE to improve understanding. However, the performance of MLLMs using discrete visual tokens on visual understanding tasks tends to be lower than mainstream models that employ continuous visual tokens. Most MLLMs with continuous visual token use CLIP features as visual input, it is a significant advantage considering that CLIP is

pre-trained on a large-scale image-text pair dataset, leading to a strong alignment between its visual space features and language space features. This alignment substantially aids the LLMs, making it easier for them to understand visual content. In contrast, using image tokens derived directly from VQVAE tokenizer as input means that the corresponding embedding features in the LLM are reinitialized with out any alignment. Without extensive pre-training to align feature spaces, the visual understanding capabilities might be slightly inferior to models using CLIP as visual input. The difference in performance mainly stems from the fact that most VQVAE currently do not align image-text spaces. VILA-U [68] has confirmed that by adding CLIP loss during the VQVAE training to align its visual space, the performance of visual understanding tasks can be improved.

However, we attempt to increase the amount of image-text pairs the model can see during the pre-training phase by training one more epoch on our multi-modal pre-training data, and then the model could achieve better performance on visual understanding tasks. This result indicates that mixed-modality pre-training plays a role similar to CLIP pre-training, aligning text and visual embedding spaces. More pret-raining or more suitable embedding initialization methods could further boost the performance of discrete visual tokens on comprehension tasks.

Table 4: Performance of pre-trained model on standard text-only benchmarks. Liquid outperforms the well-established language model LLAMA2 and the mix-pretrained multi-modal language model Chameleon in most tasks, exhibiting undegraded linguistic capabilities.

Method		BoolQ	PIQA	SIQA	HellaSwag	WinoGrande	ARC-e	ARC-c	MMLU
Mistral	7B	84.7	83.0	-	81.3	75.3	80.0	55.5	60.1
	8×7B	-	83.6	-	84.4	77.2	83.1	59.7	70.6
LLAMA2	7B	77.4	78.8	48.3	77.2	69.2	75.2	45.9	45.3
	13B	81.7	80.5	50.3	80.7	72.8	77.3	49.4	54.8
	34B	83.7	81.9	50.9	83.3	76.7	79.4	54.5	62.6
Chameleon	7B	81.4	79.6	57.0	74.2	70.4	76.1	46.5	52.1
	34B	86.0	83.3	63.3	82.7	78.5	84.1	59.7	65.8
Ours	7B	81.0	81.0	46.7	76.1	72.7	75.6	49.0	56.0

4.4 Language Tasks

We evaluate the general text-only capabilities of our pre-trained model against other state-of-the-art large language models and multi-modal language models, following the evaluation protocol of [17]. As shown in Tab. 4, Liquid outperforms the well-established language model LLAMA2 [64] and the mix-pretrained multi-modal language model Chameleon [59] in most tasks, exhibiting undegraded linguistic capabilities. Compared with Chameleon [59], which is mixed pretrained with an extremely large scale of data, Liquid performs training from existing LLMs that already possess decent language capabilities, maintaining these capabilities without degradation. This result validates the efficiency of our training framework and demonstrates that with this framework, we can extend the visual generation and understanding capabilities to LLMs of any structure and size.

4.5 Scaling Results

Benefiting from our strategy of continuing training from existing LLMs, we can conveniently scale up our model size and observe their performance on different tasks. We construct Liquid models of sizes 1B, 2B, 9B, and 27B using models from the LLAMA3.2 [14] and GEMMA2 [61]. As far as we know, no prior work has explored whether training image and text generation in a single embedding space through a single model would impact their respective performance. To explore this, we conducted three sets of experiments with the same training strategy on the four model sizes: mix image generation and text generation, text generation only, and image generation only. In mix training, we use both 30M text only and 30M image-text data introduced in Sec. 3. For text only and image only training, we only use one of them. All experiments control the batch size to 512, and the learning rate is set to a constant 2e-5. After the training is completed, we evaluate the performance of the three settings and their respective four sizes, totaling 12 models. For language ability, we evaluate two indicators, namely the zero-shot MMLU and the average zero-shot score in 5 language tasks. For

visual generation tasks, we evaluate the VQAscore on advanced prompts in GenAI-Bench. As shown in Fig. 1, we find a trade-off phenomenon when both tasks were mixed in the training of smaller models; however, as the model size increased, this trade-off gradually disappeared. This confirms that larger models possess sufficient capacity to handle both visual and language spaces generation concurrently. Furthermore, as the size of the model increases, the quality of the images generated also improves, proving that LLMs have a higher upper limit as multi-modal generators, and the same scaling-law as language models. More scaling results can be found in the supplementary materials.

4.6 Mutual Boost of Visual Generation and Understanding

In the scaling experiments, we observe that as the model size increases, the trade-off between language tasks and visual generation tasks gradually diminishes. In this section, we further explore whether there is mutual enhancement between the two tasks as the feature spaces for visual understanding and generation become unified. We conduct three sets of experiments. In the first set, we used a combination of 10M text-only data, 10M visual generation data, and 10M visual understanding data, resulting in a total of 30M data for the pre-training phase. The visual understanding data is derived by reversing the visual generation data for the captioning task, and the loss is calculated only on the text output for visual understanding task. All data are subsets of the data introduced in Section 3. The experiment, with a 1 : 1 : 1 data ratio of the three tasks, serves as the baseline. Building on this baseline, we separately add an additional 10M visual generation data and 10M visual understanding data, forming a total of 40M data with data ratios of 1 : 2 : 1 and 1 : 1 : 2, respectively, labeled as ‘Add T2I’ and ‘Add I2T’. We train three GEMMA-7B models using default parameters and evaluate their performance on visual understanding and generation tasks to observe the impact of different data additions on the performance of all tasks. For the visual understanding tasks, after the pre-training phase, we perform the same instruction tuning training and then test them on standard visual understanding benchmarks.

Method	Training Data			Visual Generation			Visual Understanding				
	Text-only	Visual Gen.	Visual Und.	Basic	Advanced	Overall	VQAv2	GQA	TextVQA	POPE	MME
Baseline	10M	10M	10M	0.63	0.58	0.60	60.7	51.3	39.2	75.9	909.6
Add T2I	10M	20M	10M	0.78	0.63	0.69	64.5	53.2	39.8	78.0	1066.8
Add I2T	10M	10M	20M	0.73	0.62	0.66	63.5	53.7	40.5	76.8	1035.1

Table 5: The impact between visual understanding and generation tasks. “Visual Gen.” refers to the data used for training text-guided image generation, while “Visual Und.” refers to the data used for training visual understanding capabilities, specifically in the form of captioning. Compared to the baseline, adding more visual understanding data enhances the visual generation capability, improving the semantic consistency between the generated content and the prompt. Conversely, increasing the visual generation data similarly aids in enhancing the model’s visual understanding ability. This indicates that when the tokens for visual generation and understanding are unified, they share a common optimization objective and can mutually enhance each other.

As shown in Tab. 5, we observe that adding more visual understanding data during pre-training significantly improves the performance of visual generation tasks. Conversely, adding more visual generation data further enhances the performance of visual understanding tasks. This important phenomenon indicates that when the modality spaces for visual understanding and generation are unified, the training of these two tasks can mutually benefit each other. Intuitively, when images are represented using embeddings from the same space, both visual generation and visual understanding tasks require stronger consistency constraints and sufficient interaction between language and visual information. Therefore, the optimization directions for these two tasks are very similar. This further demonstrates the potential of LLMs as general-purpose multi-modal generators. The continuous addition of visual training data can simultaneously enhance the models’ capabilities in both multimodal understanding and generation.

5 Conclusion

In this paper, we present Liquid, an efficient framework enabling language models to acquire image generation and understanding capabilities without modifying the original structure. Unlike traditional multi-modal models employing extra visual models, Liquid directly tokenize images into discrete

tokens that share the same embedding space with text tokens. This leads to a total unification of images and text within the models, which stokes the potential of multi-modal learning. Utilizing various existing LLMs provides a unique advantage to Liquid, enabling it to scale up easily and display similar scaling behavior to LLMs. Notably, the inherent trade-offs of unifying dual tasks within a single space diminish as the model size expands. We demonstrate that LLMs can generate high-quality images comparable to the diffusion model, and have strong potential as multi-modal generators.

References

- [1] J.-B. Alayrac, J. Donahue, P. Luc, A. Miech, I. Barr, Y. Hasson, K. Lenc, A. Mensch, K. Millican, M. Reynolds, et al. Flamingo: a visual language model for few-shot learning. *Advances in Neural Information Processing Systems*, 35:23716–23736, 2022. [4](#)
- [2] J. Bai, S. Bai, S. Yang, S. Wang, S. Tan, P. Wang, J. Lin, C. Zhou, and J. Zhou. Qwen-vl: A frontier large vision-language model with versatile abilities. *arXiv preprint arXiv:2308.12966*, 2023. [4](#)
- [3] Y. Bisk, R. Zellers, J. Gao, Y. Choi, et al. Piqa: Reasoning about physical commonsense in natural language. In *Proceedings of the AAAI conference on artificial intelligence*, pages 7432–7439, 2020. [7](#)
- [4] T. Brown, B. Mann, N. Ryder, M. Subbiah, J. D. Kaplan, P. Dhariwal, A. Neelakantan, P. Shyam, G. Sastry, A. Askell, et al. Language models are few-shot learners. *Advances in neural information processing systems*, 33:1877–1901, 2020. [1, 4](#)
- [5] G. H. Chen, S. Chen, R. Zhang, J. Chen, X. Wu, Z. Zhang, Z. Chen, J. Li, X. Wan, and B. Wang. Allava: Harnessing gpt4v-synthesized data for a lite vision-language model. *arXiv preprint arXiv:2402.11684*, 2024. [1, 4](#)
- [6] J. Chen, J. Yu, C. Ge, L. Yao, E. Xie, Y. Wu, Z. Wang, J. Kwok, P. Luo, H. Lu, et al. Pixart-alpha: Fast training of diffusion transformer for photorealistic text-to-image synthesis. *arXiv preprint arXiv:2310.00426*, 2023. [7](#)
- [7] L. Chen, J. Li, X. Dong, P. Zhang, C. He, J. Wang, F. Zhao, and D. Lin. Sharegpt4v: Improving large multi-modal models with better captions. *arXiv preprint arXiv:2311.12793*, 2023. [4](#)
- [8] A. Chowdhery, S. Narang, J. Devlin, M. Bosma, G. Mishra, A. Roberts, P. Barham, H. W. Chung, C. Sutton, S. Gehrmann, et al. Palm: Scaling language modeling with pathways. *arXiv preprint arXiv:2204.02311*, 2022. [1, 4](#)
- [9] C. Clark, K. Lee, M.-W. Chang, T. Kwiatkowski, M. Collins, and K. Toutanova. Boolq: Exploring the surprising difficulty of natural yes/no questions. *arXiv preprint arXiv:1905.10044*, 2019. [7](#)
- [10] P. Clark, I. Cowhey, O. Etzioni, T. Khot, A. Sabharwal, C. Schoenick, and O. Tafjord. Think you have solved question answering? try arc, the ai2 reasoning challenge. *arXiv preprint arXiv:1803.05457*, 2018. [7](#)
- [11] W. Dai, J. Li, D. Li, A. M. H. Tiong, J. Zhao, W. Wang, B. Li, P. Fung, and S. Hoi. Instructblip: Towards general-purpose vision-language models with instruction tuning. *arXiv*, 2023. [4, 8](#)
- [12] M. Ding, Z. Yang, W. Hong, W. Zheng, C. Zhou, D. Yin, J. Lin, X. Zou, Z. Shao, H. Yang, et al. Cogview: Mastering text-to-image generation via transformers. *Advances in neural information processing systems*, 34:19822–19835, 2021. [1, 4](#)
- [13] R. Dong, C. Han, Y. Peng, Z. Qi, Z. Ge, J. Yang, L. Zhao, J. Sun, H. Zhou, H. Wei, et al. Dreamllm: Synergistic multimodal comprehension and creation. *arXiv preprint arXiv:2309.11499*, 2023. [8](#)
- [14] A. Dubey, A. Jauhri, A. Pandey, A. Kadian, A. Al-Dahle, A. Letman, A. Mathur, A. Schelten, A. Yang, A. Fan, et al. The llama 3 herd of models. *arXiv preprint arXiv:2407.21783*, 2024. [2, 6, 9](#)
- [15] P. Esser, R. Rombach, and B. Ommer. Taming transformers for high-resolution image synthesis. In *Proceedings of the IEEE/CVF conference on computer vision and pattern recognition*, pages 12873–12883, 2021. [1, 2, 4, 5](#)
- [16] C. Fu, P. Chen, Y. Shen, Y. Qin, M. Zhang, X. Lin, J. Yang, X. Zheng, K. Li, X. Sun, Y. Wu, and R. Ji. Mme: A comprehensive evaluation benchmark for multimodal large language models, 2024. [7](#)
- [17] L. Gao, J. Tow, B. Abbas, S. Biderman, S. Black, A. DiPofi, C. Foster, L. Golding, J. Hsu, A. Le Noac'h, H. Li, K. McDonell, N. Muennighoff, C. Ociepa, J. Phang, L. Reynolds, H. Schoelkopf, A. Skowron, L. Sutawika, E. Tang, A. Thite, B. Wang, K. Wang, and A. Zou. A framework for few-shot language model evaluation, 07 2024. [9](#)
- [18] Y. Ge, Y. Ge, Z. Zeng, X. Wang, and Y. Shan. Planting a seed of vision in large language model. *arXiv preprint arXiv:2307.08041*, 2023. [1, 4](#)
- [19] Y. Ge, S. Zhao, J. Zhu, Y. Ge, K. Yi, L. Song, C. Li, X. Ding, and Y. Shan. Seed-x: Multimodal models with unified multi-granularity comprehension and generation. *arXiv preprint arXiv:2404.14396*, 2024. [1, 4](#)
- [20] Y. Goyal, T. Khot, D. Summers-Stay, D. Batra, and D. Parikh. Making the V in VQA matter: Elevating the role of image understanding in Visual Question Answering. In *Conference on Computer Vision and Pattern Recognition (CVPR)*, 2017. [7](#)
- [21] D. Hendrycks, C. Burns, S. Basart, A. Zou, M. Mazeika, D. X. Song, and J. Steinhardt. Measuring massive multitask language understanding. *arXiv preprint arXiv:2009.03300*, 2020. [7](#)
- [22] M. Heusel, H. Ramsauer, T. Unterthiner, B. Nessler, and S. Hochreiter. Gans trained by a two time-scale update rule converge to a local nash equilibrium. *Advances in neural information processing systems*, 30, 2017. [7](#)
- [23] D. A. Hudson and C. D. Manning. Gqa: A new dataset for real-world visual reasoning and compositional question answering. In *Proceedings of the IEEE/CVF conference on computer vision and pattern recognition*, pages 6700–6709, 2019. [7](#)
- [24] B. Hui, J. Yang, Z. Cui, J. Yang, D. Liu, L. Zhang, T. Liu, J. Zhang, B. Yu, K. Lu, et al. Qwen2. 5-coder technical report. *arXiv preprint arXiv:2409.12186*, 2024. [2](#)

[25] Y. Jin, K. Xu, L. Chen, C. Liao, J. Tan, B. Chen, C. Lei, A. Liu, C. Song, X. Lei, et al. Unified language-vision pretraining with dynamic discrete visual tokenization. *arXiv preprint arXiv:2309.04669*, 2023. 1, 4, 8

[26] H. Laurençon, D. van Strien, S. Bekman, L. Tronchon, L. Saulnier, T. Wang, S. Karamcheti, A. Singh, G. Pistilli, Y. Jernite, et al. Introducing idefics: An open reproduction of state-of-the-art visual language model, 2023. URL <https://huggingface.co/blog/idefics>. Accessed, pages 09–18, 2023. 8

[27] D. Li, A. Kamko, E. Akhgari, A. Sabet, L. Xu, and S. Doshi. Playground v2. 5: Three insights towards enhancing aesthetic quality in text-to-image generation. *arXiv preprint arXiv:2402.17245*, 2024. 7

[28] J. Li, A. Fang, G. Smyrnis, M. Ivgi, M. Jordan, S. Gadre, H. Bansal, E. Guha, S. Keh, K. Arora, S. Garg, R. Xin, N. Muennighoff, R. Heckel, J. Mercat, M. Chen, S. Gururangan, M. Wortsman, A. Albalak, Y. Bitton, M. Nezhurina, A. Abbas, C.-Y. Hsieh, D. Ghosh, J. Gardner, M. Kilian, H. Zhang, R. Shao, S. Pratt, S. Sanyal, G. Ilharco, G. Daras, K. Marathe, A. Gokaslan, J. Zhang, K. Chandu, T. Nguyen, I. Vasiljevic, S. Kakade, S. Song, S. Sanghavi, F. Faghri, S. Oh, L. Zettlemoyer, K. Lo, A. El-Nouby, H. Pouransari, A. Toshév, S. Wang, D. Groeneweld, L. Soldaini, P. W. Koh, J. Jitsev, T. Kollar, A. G. Dimakis, Y. Carmon, A. Dave, L. Schmidt, and V. Shankar. Datacomp-lm: In search of the next generation of training sets for language models. *arXiv preprint arXiv:2406.11794*, 2024. 6

[29] J. Li, D. Li, S. Savarese, and S. Hoi. Blip-2: Bootstrapping language-image pre-training with frozen image encoders and large language models. In *International conference on machine learning*, pages 19730–19742. PMLR, 2023. 4

[30] J. Li, D. Li, C. Xiong, and S. Hoi. Blip: Bootstrapping language-image pre-training for unified vision-language understanding and generation. In *International conference on machine learning*, pages 12888–12900. PMLR, 2022. 4

[31] R. Li, L. B. Allal, Y. Zi, N. Muennighoff, D. Kocetkov, C. Mou, M. Marone, C. Akiki, J. Li, J. Chim, Q. Liu, E. Zheltonozhskii, T. Y. Zhuo, T. Wang, O. Dehaene, M. Davaadorj, J. Lamy-Poirier, J. Monteiro, O. Shli-azhko, N. Gontier, N. Meade, A. Zebaze, M.-H. Yee, L. K. Umapathi, J. Zhu, B. Lipkin, M. Oblokulov, Z. Wang, R. Murthy, J. Stillerman, S. S. Patel, D. Abulkhanov, M. Zocca, M. Dey, Z. Zhang, N. Fahmy, U. Bhattacharyya, W. Yu, S. Singh, S. Lucioni, P. Villegas, M. Kunakov, F. Zhdanov, M. Romero, T. Lee, N. Timor, J. Ding, C. Schlesinger, H. Schoelkopf, J. Ebert, T. Dao, M. Mishra, A. Gu, J. Robinson, C. J. Anderson, B. Dolan-Gavitt, D. Contractor, S. Reddy, D. Fried, D. Bahdanau, Y. Jernite, C. M. Ferrandis, S. Hughes, T. Wolf, A. Guha, L. von Werra, and H. de Vries. Starcoder: may the source be with you! *arXiv preprint arXiv:2305.06161*, 2023. 6

[32] Y. Li, Y. Zhang, C. Wang, Z. Zhong, Y. Chen, R. Chu, S. Liu, and J. Jia. Mini-gemini: Mining the potential of multi-modality vision language models. *arXiv preprint arXiv:2403.18814*, 2024. 4, 6

[33] J. Lin, H. Yin, W. Ping, Y. Lu, P. Molchanov, A. Tao, H. Mao, J. Kautz, M. Shoeybi, and S. Han. Vila: On pre-training for visual language models, 2023. 8

[34] Z. Lin, D. Pathak, B. Li, J. Li, X. Xia, G. Neubig, P. Zhang, and D. Ramanan. Evaluating text-to-visual generation with image-to-text generation. *arXiv preprint arXiv:2404.01291*, 2024. 4, 8

[35] Z. Lin, D. Pathak, B. Li, J. Li, X. Xia, G. Neubig, P. Zhang, and D. Ramanan. Evaluating text-to-visual generation with image-to-text generation. *arXiv preprint arXiv:2404.01291*, 2024. 7

[36] H. Liu, C. Li, Y. Li, and Y. J. Lee. Improved baselines with visual instruction tuning. In *Proceedings of the IEEE/CVF Conference on Computer Vision and Pattern Recognition*, pages 26296–26306, 2024. 1, 4

[37] H. Liu, C. Li, Y. Li, B. Li, Y. Zhang, S. Shen, and Y. J. Lee. Llava-next: Improved reasoning, ocr, and world knowledge, January 2024. 1, 4

[38] H. Liu, C. Li, Q. Wu, and Y. J. Lee. Visual instruction tuning. *Advances in neural information processing systems*, 36, 2024. 1, 4, 8

[39] H. Liu, W. Yan, M. Zaharia, and P. Abbeel. World model on million-length video and language with ringattention. *arXiv preprint arXiv:2402.08268*, 2024. 2, 4, 7, 8

[40] J. Lu, C. Clark, S. Lee, Z. Zhang, S. Khosla, R. Marten, D. Hoiem, and A. Kembhavi. Unified-io 2: Scaling autoregressive multimodal models with vision language audio and action. In *Proceedings of the IEEE/CVF Conference on Computer Vision and Pattern Recognition*, pages 26439–26455, 2024. 4, 8

[41] Y. Lu, C. Li, H. Liu, J. Yang, J. Gao, and Y. Shen. An empirical study of scaling instruct-tuned large multimodal models. *arXiv preprint arXiv:2309.09958*, 2023. 1, 4

[42] T. Mihaylov, P. Clark, T. Khot, and A. Sabharwal. Can a suit of armor conduct electricity? a new dataset for open book question answering. *arXiv preprint arXiv:1809.02789*, 2018. 7

[43] J. Pan, K. Sun, Y. Ge, H. Li, H. Duan, X. Wu, R. Zhang, A. Zhou, Z. Qin, Y. Wang, J. Dai, Y. Qiao, and H. Li. Journeydb: A benchmark for generative image understanding, 2023. 6

[44] D. Podell, Z. English, K. Lacey, A. Blattmann, T. Dockhorn, J. Müller, J. Penna, and R. Rombach. Sdxl: Improving latent diffusion models for high-resolution image synthesis. *arXiv preprint arXiv:2307.01952*, 2023. 4, 7, 8

[45] A. Radford, J. W. Kim, C. Hallacy, A. Ramesh, G. Goh, S. Agarwal, G. Sastry, A. Askell, P. Mishkin, J. Clark, et al. Learning transferable visual models from natural language supervision. In *International conference on machine learning*, pages 8748–8763. PMLR, 2021. 1, 4

[46] A. M. Radhakrishnan. Is midjourney-ai the new anti-hero of architectural imagery & creativity? *GSJ*, 11(1):94–104, 2023. 4, 8

[47] C. Raffel, N. Shazeer, A. Roberts, K. Lee, S. Narang, M. Matena, Y. Zhou, W. Li, and P. J. Liu. Exploring the limits of transfer learning with a unified text-to-text transformer. *The Journal of Machine Learning Research*, 21(1):5485–5551, 2020. 1

[48] A. Ramesh, P. Dhariwal, A. Nichol, C. Chu, and M. Chen. Hierarchical text-conditional image generation with clip latents. *arXiv preprint arXiv:2204.06125*, 1(2):3, 2022. 4

[49] A. Ramesh, M. Pavlov, G. Goh, S. Gray, C. Voss, A. Radford, M. Chen, and I. Sutskever. Zero-shot text-to-image generation. In *International Conference on Machine Learning*, pages 8821–8831. PMLR, 2021. 1, 4

[50] R. Rombach, A. Blattmann, D. Lorenz, P. Esser, and B. Ommer. High-resolution image synthesis with latent diffusion models. In *Proceedings of the IEEE/CVF conference on computer vision and pattern recognition*, pages 10684–10695, 2022. 4, 7, 8

[51] K. Sakaguchi, R. L. Bras, C. Bhagavatula, and Y. Choi. Winogrande: An adversarial winograd schema challenge at scale. *Communications of the ACM*, 64(9):99–106, 2021. 7

[52] M. Sap, H. Rashkin, D. Chen, R. LeBras, and Y. Choi. Socialqa: Commonsense reasoning about social interactions. *arXiv preprint arXiv:1904.09728*, 2019. 7

[53] R. Sennrich, B. Haddow, and A. Birch. Neural machine translation of rare words with subword units. In K. Erk and N. A. Smith, editors, *Proceedings of the 54th Annual Meeting of the Association for Computational Linguistics (Volume 1: Long Papers)*, pages 1715–1725, Berlin, Germany, Aug. 2016. Association for Computational Linguistics. 2, 5

[54] A. Singh, V. Natarajan, M. Shah, Y. Jiang, X. Chen, D. Batra, D. Parikh, and M. Rohrbach. Towards vqa models that can read. In *Proceedings of the IEEE/CVF conference on computer vision and pattern recognition*, pages 8317–8326, 2019. 7

[55] D. Soboleva, F. Al-Khateeb, R. Myers, J. R. Steeves, J. Hestness, and N. Dey. SlimPajama: A 627B token cleaned and deduplicated version of RedPajama. <https://www.cerebras.net/blog/slimpajama-a-627b-token-cleaned-and-deduplicated-version-of-redpajama>, 2023. 6

[56] P. Sun, Y. Jiang, S. Chen, S. Zhang, B. Peng, P. Luo, and Z. Yuan. Autoregressive model beats diffusion: Llama for scalable image generation. *arXiv preprint arXiv:2406.06525*, 2024. 1, 4

[57] Q. Sun, Y. Cui, X. Zhang, F. Zhang, Q. Yu, Y. Wang, Y. Rao, J. Liu, T. Huang, and X. Wang. Generative multimodal models are in-context learners. In *Proceedings of the IEEE/CVF Conference on Computer Vision and Pattern Recognition*, pages 14398–14409, 2024. 1, 4

[58] Q. Sun, Q. Yu, Y. Cui, F. Zhang, X. Zhang, Y. Wang, H. Gao, J. Liu, T. Huang, and X. Wang. Generative pretraining in multimodality. *arXiv preprint arXiv:2307.05222*, 2023. 1, 4, 8

[59] C. Team. Chameleon: Mixed-modal early-fusion foundation models. *arXiv preprint arXiv:2405.09818*, 2024. 2, 4, 5, 8, 9

[60] G. Team, T. Mesnard, C. Hardin, R. Dadashi, S. Bhupatiraju, S. Pathak, L. Sifre, M. Rivière, M. S. Kale, J. Love, et al. Gemma: Open models based on gemini research and technology. *arXiv preprint arXiv:2403.08295*, 2024. 1, 2, 4, 5

[61] G. Team, M. Riviere, S. Pathak, P. G. Sessa, C. Hardin, S. Bhupatiraju, L. Hussenot, T. Mesnard, B. Shahriari, A. Ramé, et al. Gemma 2: Improving open language models at a practical size. *arXiv preprint arXiv:2408.00118*, 2024. 2, 5, 6, 9

[62] K. Tian, Y. Jiang, Z. Yuan, B. Peng, and L. Wang. Visual autoregressive modeling: Scalable image generation via next-scale prediction. *arXiv preprint arXiv:2404.02905*, 2024. 1, 4

[63] H. Touvron, T. Lavril, G. Izacard, X. Martinet, M.-A. Lachaux, T. Lacroix, B. Rozière, N. Goyal, E. Hambro, F. Azhar, et al. Llama: Open and efficient foundation language models. *arXiv preprint arXiv:2302.13971*, 2023. 1, 4

[64] H. Touvron, L. Martin, K. Stone, P. Albert, A. Almahairi, Y. Babaei, N. Bashlykov, S. Batra, P. Bhargava, S. Bhosale, et al. Llama 2: Open foundation and fine-tuned chat models. *arXiv preprint arXiv:2307.09288*, 2023. 1, 4, 9

[65] A. Van Den Oord, O. Vinyals, et al. Neural discrete representation learning. *Advances in neural information processing systems*, 30, 2017. 1

[66] Y. Wang, T. Xiong, D. Zhou, Z. Lin, Y. Zhao, B. Kang, J. Feng, and X. Liu. Loong: Generating minute-level long videos with autoregressive language models. *arXiv preprint arXiv:2410.02757*, 2024. 4

[67] C. Wu, X. Chen, Z. Wu, Y. Ma, X. Liu, Z. Pan, W. Liu, Z. Xie, X. Yu, C. Ruan, et al. Janus: Decoupling visual encoding for unified multimodal understanding and generation. *arXiv preprint arXiv:2410.13848*, 2024. 4, 7

[68] Y. Wu, Z. Zhang, J. Chen, H. Tang, D. Li, Y. Fang, L. Zhu, E. Xie, H. Yin, L. Yi, et al. Vila-u: a unified foundation model integrating visual understanding and generation. *arXiv preprint arXiv:2409.04429*, 2024. 2, 4, 7, 8, 9

[69] J. Xie, W. Mao, Z. Bai, D. J. Zhang, W. Wang, K. Q. Lin, Y. Gu, Z. Chen, Z. Yang, and M. Z. Shou. Show-o: One single transformer to unify multimodal understanding and generation. *arXiv preprint arXiv:2408.12528*, 2024. 2, 4, 7, 8

- [70] A. Yang, B. Xiao, B. Wang, B. Zhang, C. Bian, C. Yin, C. Lv, D. Pan, D. Wang, D. Yan, et al. Baichuan 2: Open large-scale language models. *arXiv preprint arXiv:2309.10305*, 2023. 6
- [71] J. Yu, Y. Xu, J. Y. Koh, T. Luong, G. Baid, Z. Wang, V. Vasudevan, A. Ku, Y. Yang, B. K. Ayan, et al. Scaling autoregressive models for content-rich text-to-image generation. *arXiv preprint arXiv:2206.10789*, 2(3):5, 2022. 1, 4
- [72] L. Yu, B. Shi, R. Pasunuru, B. Muller, O. Golovneva, T. Wang, A. Babu, B. Tang, B. Karrer, S. Sheynin, et al. Scaling autoregressive multi-modal models: Pretraining and instruction tuning. *arXiv preprint arXiv:2309.02591*, 2(3), 2023. 8
- [73] R. Zellers, A. Holtzman, Y. Bisk, A. Farhadi, and Y. Choi. Hellaswag: Can a machine really finish your sentence? *arXiv preprint arXiv:1905.07830*, 2019. 7
- [74] L. Zheng, W.-L. Chiang, Y. Sheng, T. Li, S. Zhuang, Z. Wu, Y. Zhuang, Z. Li, Z. Lin, E. P. Xing, et al. Lmsys-chat-1m: A large-scale real-world llm conversation dataset. *arXiv preprint arXiv:2309.11998*, 2023. 6
- [75] C. Zhou, L. Yu, A. Babu, K. Tirumala, M. Yasunaga, L. Shamis, J. Kahn, X. Ma, L. Zettlemoyer, and O. Levy. Transfusion: Predict the next token and diffuse images with one multi-modal model. *arXiv preprint arXiv:2408.11039*, 2024. 2
- [76] D. Zhu, J. Chen, X. Shen, X. Li, and M. Elhoseiny. Minigpt-4: Enhancing vision-language understanding with advanced large language models. *arXiv preprint arXiv:2304.10592*, 2023. 1, 4